**PATTERN FORMATION IN A TYPE-II OPTICAL PARAMETRIC OSCILLATOR**

by

Gonzalo Izús[1], Marco Santagiustina[2], Maxi San Miguel[1], Pere Colet[1]

[1] : *Instituto Mediterráneo de Estudios Avanzados, IMEDEA (CSIC-UIB) E-07071 Palma de Mallorca, Spain.*
[2] : *Istituto Nazionale di Fisica della Materia, Dipartimento di Elettronica ed Informatica, Università di Padova, via Gradenigo 6/a, 35131 Padova, Italy.*

## Abstract

We show the relevance of walk-off and birefringence/dichroic effects in pattern formation in a type-II optical parametric oscillator (OPO). Walk-off generates a convectively unstable regime in which we show the existence of intensity patterns sustained by noise. The patterns arise form the interference between traveling waves which are excited by noise and dynamically amplified. As another example of pattern formation in type-II OPO's, we show that the presence of a birefringent and/or dichroic mirror yields to a new kind of domain walls. In these walls the field amplitude does not vanishes at the core of the wall while the phase rotates when going from one domain to the neighboring one. These domain walls are similar to Bloch walls in magnetic systems. They appear spontaneously here for positive or null detunings, where the zero wavenumber is selected.

## 1 Introduction

Pattern formation in many nonlinear optical systems has been an active field of investigation [1]. New experiments on spatial modulational instability in bulk quadratic media [2] clearly indicate that pattern formation in optical parametric oscillators, theoretically predicted [3], could be experimentally observed.

An important characteristic of OPO's is that the anisotropy can cause the Poynting vectors of the extraordinary polarized components to walk-off the ordinary ones (double-refraction phenomenon) in the plane transverse to the propagation direction. In a type-II OPO's the down-converted beams are polarized along both the ordinary and extraordinary axes, i.e. are polarization non-degenerate. Here, we study the effects introduced by: a) the walk-off and b) the birefingence/dichroism of one mirror of the cavity in the process of pattern formation in a type-II OPO.

## 2 Governing equations

The equations describing the time evolution of the normalized slowly varying envelopes of the transverse second harmonics (SHs) $A_{0,0'}(\vec{r},t)$ and the fundamental harmonics (FHs) $A_{1,2}(\vec{r},t)$ electric fields for a type-II, phase-matched, ring, frequency non-degenerate OPO (NDOPO) in the mean-field approximation can be derived in a similar way as those of ref. [4]:

$$\begin{aligned}
\partial_t A_{0'} &= \gamma_{0'}[-(1+i\Delta_{0'})A_{0'} + ia_{0'}\nabla^2 A_{0'} + c_{0'}\,A_0] + \sqrt{\epsilon_{0'}}\,\xi_{0'}(\vec{r},t) \\
\partial_t A_0 &= \gamma_0[-(1+i\Delta_0)A_0 + E_0 + ia_0\nabla^2 A_0 + 2iK_0A_1A_2 + c_0\,A_{0'}] + \sqrt{\epsilon_0}\,\xi_0(\vec{r},t) \\
\partial_t A_1 &= \gamma_1[-(1+i\Delta_1)A_1 + ia_1\nabla^2 A_1 + iK_0A_2^*A_0 + c_1\,A_2] + \sqrt{\epsilon_1}\,\xi_1(\vec{r},t) \\
\partial_t A_2 &= \gamma_2[-(1+i\Delta_2)A_2 + \rho\,\partial_y A_2 + ia_2\nabla^2 A_2 + iK_0A_1^*A_0 + c_2\,A_1] + \sqrt{\epsilon_2}\,\xi_2(\vec{r},t) \qquad (1)
\end{aligned}$$

where we are considering that one of the mirrors into the linear cavity is birefringent/dichroic. Here $A_{0,1}$ are ordinary polarized beams and $A_{0',2}$ are extraordinary polarized; $\vec{r}=(x,y)$ is the transversal spatial vector, $t$ is the time and $\gamma_j$ , $\Delta_j$ and $a_j$ are respectively the cavity decay rate, detuning and diffraction for the field $A_j$. The nonlinear coefficient is $K_0$, $E_0$ is the injected pump and $\rho$ is the walk-off coefficient. The linear coupling coefficients $c_{0,0'}$, $c_{1,2}$ are related to the dichroism and the the birefringence of the mirror [5]. The last term of each equation is an independent complex Gaussian white noise with zero mean value and delta-correlated in space and time. These terms describe quantum noise in the Wigner representation for the linearized version of eqs.(1) [7], but they can account for thermal or input fluctuations as well.

## 3 Walk-off effects

We consider first the case in wich $c_{0,0'}$, $c_{1,2}=0$, that is there not a birefringent-dichroic mirror into the optical cavity and we concentrate in the fields $A_{0,1,2}$. In this case eqs.(1) have the uniform steady state solution $A_0 = E_0/(1+i\Delta_0)$, $A_1 = A_2 = 0$. A linear stability analysis determines that $A_{0,0'}$ is always stable while $A_1$ and $A_2^*$ become unstable if the normalized pump intensity $F = K_0E_0/(1+i\Delta_0)$ is such that:

$$|F|^2 \geq 1 + \left[\frac{q^2\tilde{a} + \tilde{\Delta} + \gamma_2\rho q_y}{\gamma_1+\gamma_2}\right]^2 \qquad (2)$$

The critical threshold value $|F_c| = 1$ corresponds to traveling waves $A_1, A_2^* \simeq \exp[i\vec{q}\vec{r} + \lambda(\vec{q})\,t]$, whose two-dimensional real wave-vector $\vec{q}$ belongs to a circle centered at $\vec{q}_0 = (0, q_{0,y})$ with radius $R = |\vec{q}-\vec{q}_0| = \sqrt{q_{0,y}^2 - \tilde{\Delta}/\tilde{a}}$, where $q_{0,y} = -\gamma_2\rho/2\tilde{a}$, $\tilde{a} = \gamma_1 a_1 + \gamma_2 a_2$, and $\tilde{\Delta} = \gamma_1\Delta_1 + \gamma_2\Delta_2$. Without walk-off the rings of the most unstable modes for $A_1$ and $A_2$ would overlap and, for $|F| > |F_c|$, any $\vec{q}$ mode on the ring, and the opposite for the orthogonal component, can be selected by spontaneous symmetry breaking. Hence a phase pattern appears in $A_1$ and $A_2$ while the intensity in both polarizations remains homogeneous [6].

Pattern formation requires $R > 0$ which only occurs for $\tilde{\Delta} < 0$ when $\rho = 0$. The walk-off shifts the center of the rings along the direction of the advection term in opposite directions

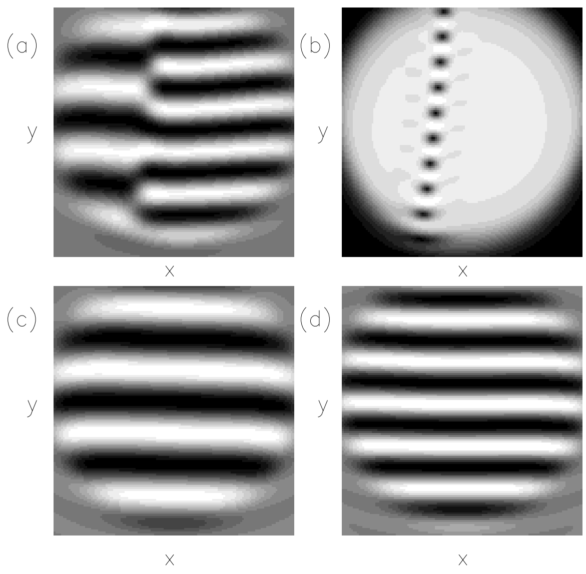


Fig. 1 Transient competition between the most unstable modes a) $\Re(A_1)$, b) $|A_1|^2$; c) and d) show $\Re(A_1)$ for the final state where the largest or shortest wavelength structure has been selected. Parameters are $2a_0 = a_{1,2} = 0.25, \gamma_{0,1,2} = 1, \Delta_0 = 0, \Delta_{1,2} = -0.15, K_0 = 1, \rho = 0.15$; $E_0$ is a super-Gaussian beam of maximum amplitude $E_{max} = 1.05$.

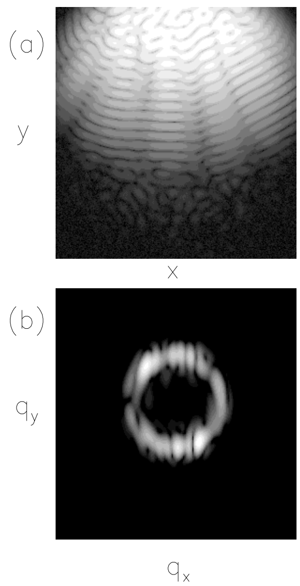


Fig. 2 Intensity of polarization component $A_1$ in the a) near field and b) far field in the convectively unstable regime. Parameters as in fig. 1 except for $\epsilon_0 = \epsilon_1 = \epsilon_2 = 2 \times 10^{-13}$, $\Delta_{1,2} = -0.2$ and $E_{max} = 1.009$.

for $A_1$ and $A_2$ and also increases their radius $R$. The shift appears on both rings because of conservation of photon momentum which has no transverse component for the input SH. Finally, the walk-off induces the pattern to drift and breaks the rotational symmetry so that the selected wave-vector orientation is parallel to the walk-off direction.

The transversal drift induced by the walk-off can overcome the spreading velocity of the unstable modes that form the pattern, so that the pattern is effectively washed out of the system: this is the convectively unstable regime, which is found for pump amplitudes up to the absolutely instability threshold $|F_a|$. This threshold can be determined by extending the linear analysis to complex wave-vectors $\vec{k}$ [4, 8, 9] (formally equivalent to the substitution $i\vec{q} \to \vec{k}$).

There are two modes for which $A_1$ and $A_2^*$ become absolutely unstable at the threshold of absolute instability $|F| = |F_a|$. These correspond to two equally likely to be selected phase patterns with different wavelength and oriented perpendicularly to the $y$-axis [10]. For large enough systems, and starting from random initial conditions there is a transient regime in which a competition between these two wave-vectors takes place as shown in fig.1a. The $\Re(A_1)$ shows stripes perpendicular to the drift direction while the intensity $|A_1|^2$ is homogeneous in each of the regions dominated by a given wavelength. The front between these regions displays a set of vertically ordered defects (fig.1b). The field $A_2^*$ displays a pattern identical to that shown for

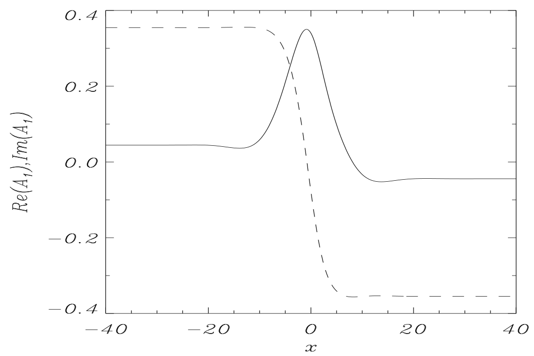


Fig.3 A numerical solution of eqs.(1), in one spatial dimension, showing a Bloch wall. Solid line represents the real part of $A_1$ and the dotted line the imaginary one. The parameters are $\gamma_1 = \gamma_{1'} = 1$, $\gamma_2 = \gamma_{2'} = 1.002$, $\Delta_{1'} = \Delta_{2'} = 0$, $\Delta_1 = 0.01$, $\Delta_2 = 0.03$, $a_{1'} = a_{2'} = 0.125$, $a_1 = a_2 = 0.25$, $K_0 = 1$, $E = 1.25$, $c_0 = c_{0'} = 0.025(1 - i/2)$ and $c_1 = c_2 = 0.02i$.

$A_1$. For long time one of the two wave-vectors is selected, as shown in fig.1c and fig.1d.

In the convectively unstable regime noise-sustained structures are expected. These structures are locally sustained because, although advected away, they are continuously regenerated by noise which at each space point excites all the unstable modes of each polarization [4]. In particular the most rapidly spreading modes can interfere generating intensity stripes as shown in the numerical solution of fig.2a. The active modes in this regime can be seen in fig.2.b (far field). The existence of patterns in the intensity is a completely new feature for a type-II OPO, due to the interplay of the convective nature of the instability (i.e. the walk-off) and the presence of noise [10].

# 4 Birefringent/dichcoic effects

In this section we consider the case in which there is neither walk-off nor noise $\rho = \epsilon_i = 0$ but now one of the cavity mirrors is birefringent-dichroic: $c_{0,0'}, c_{1,2} \neq 0$. A linear stability analysis shows that the trivial solution $A_{1,2} = 0$, $A_0 = (1 + i\Delta_{2'})E_0/(1 - \Delta_{1'}\Delta_{2'} - c_0 c_{0'} + i(\Delta_{1'} + \Delta_{2'}))$, $A_{0'} = c_{0'}E_0/(1 - \Delta_{1'}\Delta_{2'} - c_0 c_{0'} + i(\Delta_{1'} + \Delta_{2'}))$, is stable for $E_0 < E_c$ where $E_c = (1 + i\Delta_1)\sqrt{1 + (\frac{\widetilde{\Delta}}{\gamma_1 + \gamma_2})^2}$, $\widetilde{\Delta} > 0$, if $c_{0,0'}$, $c_{1,2} = 0$. No analytical solution could be found for $c_{0,0'}$, $c_{1,2} \neq 0$, but $E_c$ could be determined through numerical solutions. For $\widetilde{\Delta} > 0$ homogeneous perturbations have the largest growth rate. In this case two homogeneous solutions $A^+_{1,2}$ and $A^-_{1,2}$ of equal amplitude and phase-shifted by $\pi$ radiants ($A^+_{1,2} = -A^-_{1,2}$) bifurcate from $A_1 = A_2 = 0$, having the same probability to be selected starting from random initial conditions. Numerical integrations of eqs.(1) confirm that stationary uniform domains, where $A_{1,2}$ are either $A^+_{1,2}$ and $A^-_{1,2}$, form spontaneously: for small values of $c_{1,2}$ separating fronts are of the Bloch type while for larger values they are of the Ising type. In fig.3 an example of a one-dimensional (1D) Bloch wall

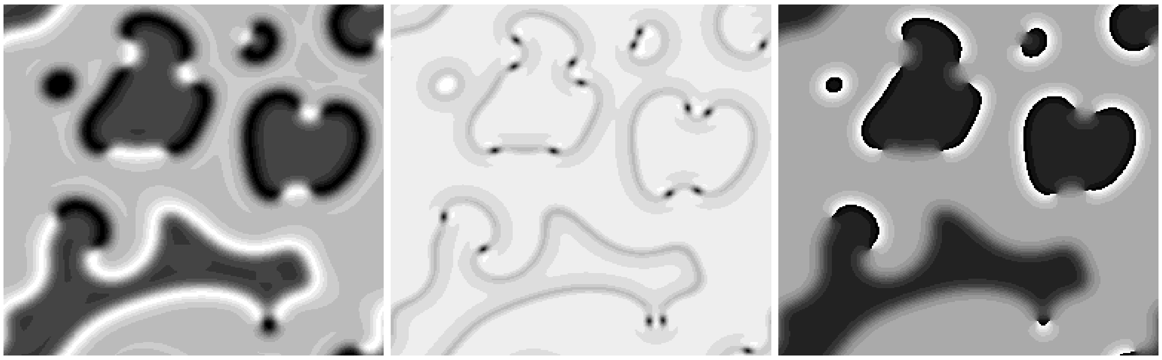

(a) (b) (c)

Fig.4 A snapshot at time t=1600 of the field $A_1(x, y, t)$ which appear spontaneously from random initial conditions. Respectively a) real part; b) intensity and c) phase. Black and white segments in the walls in fig. 4a correspond to opposite sense of rotations of the phase (chirality). The black points in fig. 4b are the defects where signal and idler vanish. They appear at points of the Bloch walls where chirality changes sign. The parameters are $\gamma_{1'} = \gamma_2 = 1$, $\gamma_{2'} = \gamma_1 = 1.002$, $\Delta_{1'} = \Delta_{2'} = 0$, $\Delta_1 = 0.01$, $\Delta_2 = 0.03$, $E = 1.25$, $a_{1'} = a_{2'} = 0.125$, $a_1 = a_2 = 0.25$, $K_0 = 1$, $c_0 = c_{0'} = 0.025(1 + i/2)$ and $c_1 = c_2 = 0.02(1 + i)$.

for $A_1$ is shown. The phase can rotates in two possible senses (chirality) across the interface, clockwise or counterclockwise in the complex plane. The wall for $A_2$ has the opposite chirality.

In two dimensions (2D) the domain walls that grow from random initial conditions can emerge with opposite chirality in different spatial regions. The change of chirality takes place in singular points, where the phase field is not defined and the amplitude is zero (defects), as we show in fig.4. Observe, in fig.4a, the interfaces that separate $A^+_{1,2}$ from $A^-_{1,2}$ (the homogeneous regions); walls of different chirality are represented respectively by the black or white thick curves. Defects associated with the changes of chirality are observed as black dots in the intensity field (fig.4b) while the phase field is shown in fig.4c. Similar structures have been reported in the description of the ordering process of a nonconserved anisotropic XY-spin system in 2D [11]. The dynamics of Bloch walls in 2D can be of two types, depending on the detuning and damping values, and it is influenced by the curvature of the walls themselves. For $\gamma_1\Delta_1 = \gamma_2\Delta_2$ flat Bloch walls are stable (this can be checked by observing that 1D walls do not move for the same parameters); then, the ordering process is mainly controlled by the curvature of the fronts. This leads to the growth of a phase at the expenses of the other and the annihililation of all the defects. For $\gamma_1\Delta_1 \neq \gamma_2\Delta_2$ walls of different chirality move in opposite directions in a 1D system. Then, in 2D, the defects are notably stable and the Bloch walls of different chirality tend to spiral around them. The fronts of equal chirality annihilate, when they collide, and new ones are generated by the defects (fig.5). The wall width diverges to infinity as $c_{1,2} \to 0$ and Bloch walls are not stable for $c_{1,2} = 0$. In fact when coupling is removed phase invariance is restored into eqs. (1). However, note that even a small amount of birefringence or dichroism is sufficient to make these structures stable and therefore they are likely to be observed in Type-II OPO's, due to any weak imperfection of the cavity.

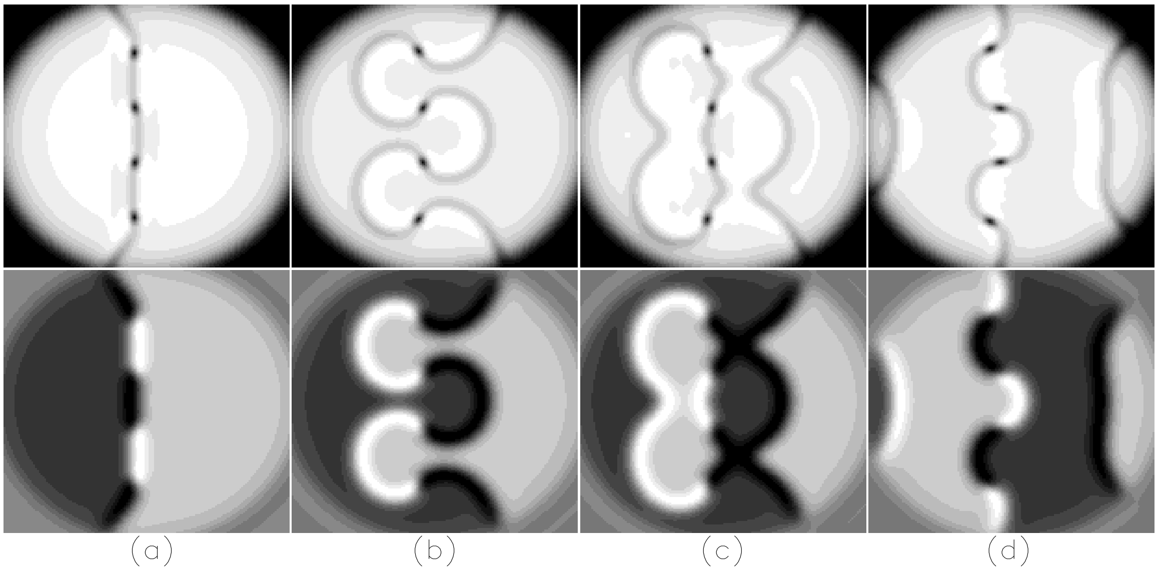


Fig.5. Time evolution of a Bloch wall: a) t=0; b) t=1000; c) t=1150; d) t=1550. Above: intensity patterns for $A_1$, below: the corresponding real part. The parameters are: $\gamma_{1'} = \gamma_2 = 1$, $\gamma_{2'} = \gamma_1 = 1.002$, $\Delta_{1'} = \Delta_{2'} = 0$, $\Delta_1 = 0.01$, $\Delta_2 = 0.03$, $E = 1.25$, $a_{1'} = a_{2'} = 0.125$, $a_1 = a_2 = 0.25$, $K_0 = 1$, $c_0 = c_{0'} = 0.01$ and $c_1 = c_2 = 0.025$. This array of defects generate an ordered spatio-temporal structure which produces (far from the defects) a sucesion of Bloch walls of opposite chirality.

# 5 Summary

In conclusion, we have studied the influence of birefringence/dichroism in the pattern formation of a type-II OPO in two cases.

First we have considered the effect of walk-off, which induces the presence of absolutely and convectively unstable regimes. In the absolutely unstable regime phase stripes have been numerically observed, the wavelength being randomly selected out of two possible different values. The difference in the wave-vector stems directly from the walk-off. An initial regime of wave-vector competition is also observed. In the convectively unstable regime it has been demonstrated that noise-sustained structures of intensity can be observed.

Second, in the case of birefringent/dichroic cavity mirror, we show the existence of Bloch walls in type-II optical parametric oscillators. They appear when there exists a small linear coupling between the signal and the idler that stems from the birefringence and/or dichroism of the cavity mirrors.

This work is supported by the European Commission through the Project QSTRUCT (ERB FMRX-CT96-0077). Financial support from DGESIC (Spain) Projects PB94-1167 and PB97-0141-02-C02 is also acknowledged. MSM acknowledges useful discussions with P. Glorieux and M. Taki.

## References


[1] L. A. Lugiato, M. Brambilla and A. Gatti, Optical Pattern Formation, in Advances in Atomic Molecular and Optical Physics, ed. by B. Bederson and H. Walther, Academic Press, to be published, and therein references.

[2] R.A. Fuerst, D-M Baboiu, B.Lawrence, W.E Torruelas, G.I. Stegeman, S. Trillo, Phys. Rev. Lett. **78**, 2756 (1997).

[3] K. Staliunas, Opt. Comm. **91**, 82 (1992). G-L. Oppo, M. Brambilla, L.A. Lugiato, Phys. Rev. A **49**, 2028 (1994). S. Longhi, J. Mod. Opt. **43**, 1089 (1996). G.J. de Varcarcel, K. Staliunas, E. Roldan, V.J. Sanchez-Morcillo, Phys. Rev. A **54**, 1609 (1996).

[4] M. Santagiustina, P. Colet, M. San Miguel and D. Walgraef, Phys. Rev. E **58**, 3843 (1998).

[5] G. Izús, M. Santagiustina and M. San Miguel, Optics Letters, in press (2000).

[6] S. Longhi, Phys. Rev. A **53**, 4488 (1996).

[7] A. Gatti, H. Wiedemann, L. A. Lugiato, I. Marzoli, G. L. Oppo and S. M. Barnett, Phys. Rev. A **56**, 877 (1997).

[8] M. Santagiustina, P. Colet, M. San Miguel, D. Walgraef, Phys. Rev. Lett. **79**, 3633 (1997).

[9] R.J. Deissler, J. Stat. Phys. **40**, 376 (1985); **54**, 1459 (1989); Physica D **56**, 303 (1992).

[10] G. Izús, M. Santagiustina, M. San Miguel, P. Colet, J. Opt. Soc. Am. B **16**, 1592 (1999).

[11] H. Tutu, Phys. Rev. E **56**, 5036 (1997).